A Numerical Study of the Steady Circulation in an Open Bay[1]

YA HSUEH AND CHICH-YUAN PENG

Dept. of Oceanography and Geophysical Fluid Dynamics Institute, Florida State University, Tallahassee 32306

(Manuscript received 21 September 1972, in revised form 30 November 1972)

ABSTRACT

The steady-state circulation in a rectangular bay is studied numerically in a model of homogeneous water and vertical coasts. The competing influences of the surface winds and longshore currents flowing by the open side of the bay and the effect of the bathymetry are emphasized. For a wind-stress field that does not vary along the coast but decays linearly inshore from the open side of the bay, the mass-transport streamfunction contours form a gyre rotating in the sense of the wind-stress curl. A uniform continental shelf slope distorts the gyre by creating depth variations that cause vortex stretching. Consequently, the streamlines become more packed to the right of the down-slope direction. The nonlinearity tends to destroy symmetry by crowding streamlines in the direction of the induced current. The influence of large-scale ocean currents along the open side is normally confined to the outer half of the bay. When the wind is blowing against these currents, the influence of the wind creates two gyres, one each at the inshore corners of the bay.

1. Introduction

An open bay represents an important near-shore portion of the continental shelf water. The circulation patterns in the bay influence many pollution and ecological problems in dictating the dispersion characteristics of contaminants which are often released directly into the bay area. The indent section between Cape San Blas and Tarpon Springs along the West Florida Gulf Coast is but one example of such a system (see Fig. 1). The hydrodynamics of a body of water of this size is certainly affected by the rotation of the earth, but for all practical purposes, not by the curvature of the earth. As such, it represents one of the rare instances when the f-plane approximation becomes quite applicable. The primary sources of energy for the generation of currents in such a system are, of course, the tides, the density gradients, the winds, and the large-scale ocean currents along the open side. In the present study, only the response to the last two forms of driving mechanism will be considered. The model is homogeneous in density. This corresponds roughly to the situation that exists over the West Florida continental shelf during late winter and early spring when the shelf water is well mixed.

Studies that are comparable to the one described here are to be found in literature in connection with the Great Lakes (Rao and Murty, 1970), but the nonlinearity that is inherent in the primitive equations and the lateral friction that becomes important in a small semi-enclosed body of water are generally ignored. The present work attempts to include all these additional effects. The vertical component of the vorticity equation in terms of the mass transport streamfunction is first integrated with the alternating direction implicit (ADI) method (Conte and Dames, 1958). The surface elevation anomaly is then mapped by numerically solving a Poisson equation with the method of successive over-relaxation (SOR). In future studies, the three-dimensional structure of the circulation and the joint effect of bottom topography and baroclinicity will be considered.

2. Formulation

Consider a rectangular open bay of vertical banks. Let the y^* axis be along the length of the bay and coincident with the coast and let the x^* axis point offshore. The z^* axis is positive upward from the undisturbed sea level. (For the area indicated along the West Florida Gulf Coast, the x^* axis runs roughly along the northern bank and the y^* axis will be pointing to the south in the general direction of the coastline.) At the water surface, a wind stress T_y^* in the y^* direction only is prescribed, i.e.,

$$T_y^* = T_0^* x^*/b^*. \tag{1}$$

The hypothetical distribution (1) possesses a maximum (or minimum) T_0^* at the open side ($x^*=b^*$) and vanishes at the coast. It implies a uniform wind-stress curl, T_0^*/b^*, which generates net transports. The asterisks indicate dimensional quantities. The symbol b^* represents the total width of the model bay of which c^* and d^* are the length and depth, respectively.

For a homogeneous body of water, the steady-state vorticity equation governing the nondivergent horizontal mass transports then takes the following

[1] Contribution No. 78 of the Geophysical Fluid Dynamics Institute, Florida State University.

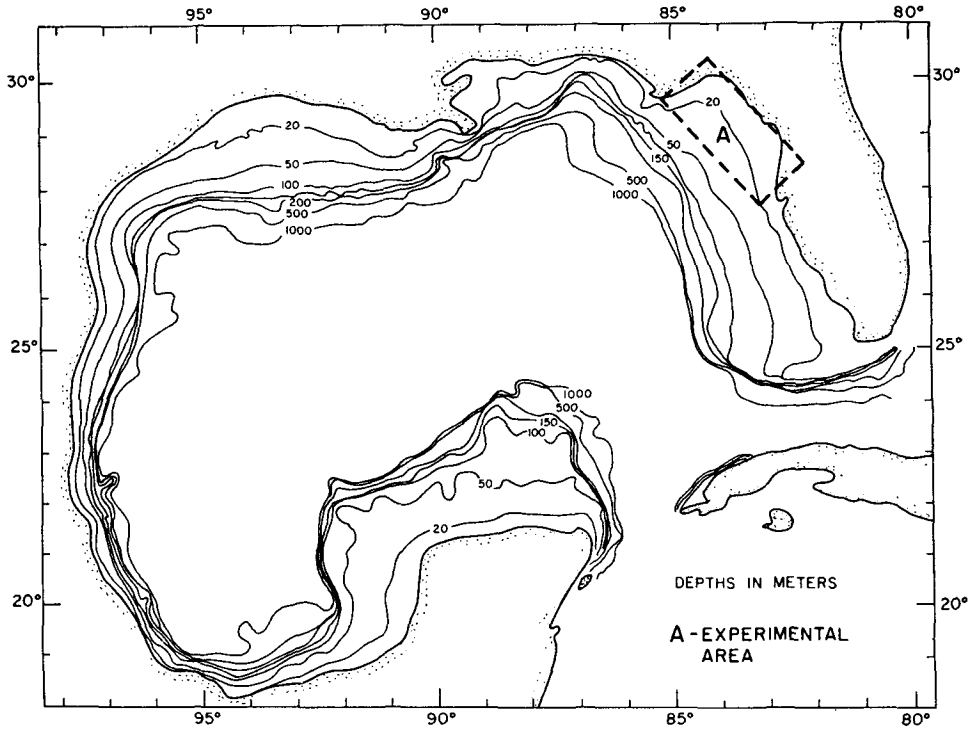

FIG. 1. Location map for the experimental area.

dimensionless form:

$$\nabla^4\phi-\gamma\nabla^2\phi-d^{-1}\,\mathrm{Ro}J(\phi,\nabla^2\phi)+d^{-1}J(\phi,d) =-b^{-1}+(bd)^{-1}ex. \quad (2)$$

The symbol ϕ stands for the streamfunction. The offshore transport S_x can be obtained by taking the negative of the derivative of ϕ with respect to y, and the transport S_y along the length of the bay can be obtained by simply taking the derivative of ϕ with respect to x. The Greek letter γ stands for a bottom friction coefficient, while d represents the scaled water depth which varies linearly from a at the coast to $a+ex$ at any other point of interest. Finally, b^{-1} represents the scaled wind-stress curl, and J stands for the Jacobian.

In arriving at (2), the terms involving the bottom slope in the nonlinear terms, and the lateral and bottom friction have been neglected. From the left, the successive terms in (2) represent the effects of lateral friction, bottom friction, advection, bottom topography, wind-stress curl, and the joint effect of the bottom topography and the wind-stress itself.

The scales that are involved in the above nondimensionalization are as follows:

$\lvert T_0^*\rvert$	wind-stress amplitude (dyn cm^{-2})
$C=\lvert T_0^*\rvert/[\rho(A_V f)^{\frac{1}{2}}]$	wind-drift speed (cm sec^{-1})
$(A_V/f)^{\frac{1}{2}}$	Ekman layer thickness (cm), a scale for vertical distances z^*, d^*, etc.
$(A_H/f)^{\frac{1}{2}}$	scale (cm) for horizontal distances x^*, y^*, etc.
$(A_V/f)^{\frac{1}{2}}C$	scale (cm^2 sec^{-1}) for the transports
$(A_V A_H)^{\frac{1}{2}}C/f$	scale (cm^3 sec^{-1}) for the streamfunction
$\mathrm{Ro}=C/(A_H f)^{\frac{1}{2}}$	Rossby number.

Here, ρ, A_V and A_H are, respectively, the density (gm cm^{-3}), and the vertical and lateral eddy viscosities (cm^2 sec^{-1}).

The boundary conditions along the three coastal boundaries for solving (2) are:

(i) At the northern and southern banks ($y=0$ and $y=c$)

$$\phi=\partial\phi/\partial y=0.$$

(ii) At the coast ($x=0$)

$$\phi=\partial\phi/\partial x=0.$$

Along the line ($x=b$) where the open shelf is joined, two kinds of boundary conditions must be considered according to whether the bay circulation is locally wind-driven or driven in part by the large-scale currents out on the open shelf. In the former situation, it seems reasonable to assume that the disturbance dies away outward from the open end. This can be simulated by taking at $x=b$ the following conditions:

(iii)
$$\left.\begin{aligned}\partial S_x/\partial x&=-\alpha S_x\\ \partial S_y/\partial x&=-\alpha S_y\end{aligned}\right\}.$$

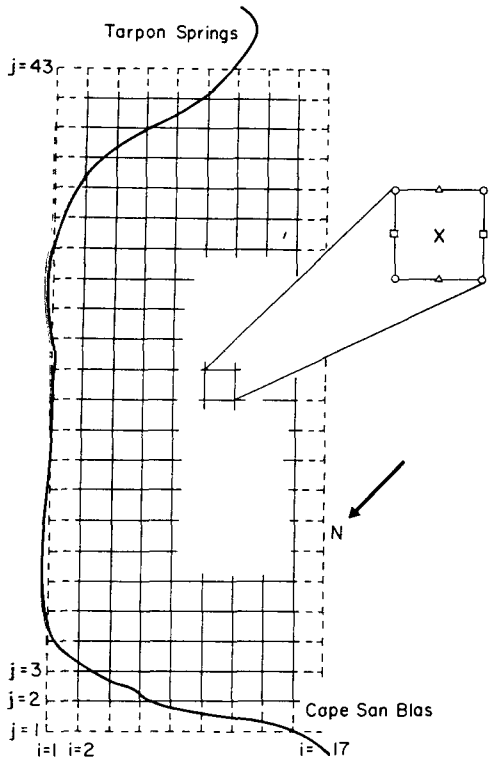

FIG. 2. The grid for numerical computation. The open circles indicate where ϕ is computed, the squares and triangles, respectively, where S_x and S_y are computed, and the cross where ζ is computed.

[As it turns out, a value of 10^{-1} of the positive constant α of proportionality gives rise to a weak shear of 10^{-7} compared with the Coriolis parameter f $(=10^{-4})$.] This formulation permits the exchange of waters between the bay and the open shelf to be determined by the dynamical equations solved within the bay. In a sense, the wind-driven bay circulation then forces the circulation over the continental shelf.

For the situation of shelf-water driving, the longshore currents at the open side of the bay must be specified:

$$\text{(iv)} \qquad \left.\begin{aligned} S_x &= 0 \\ S_y &= Q\sin(\pi y/c), \quad Q>0 \end{aligned}\right\}.$$

The occasion when (iv) may become applicable arises, for instance, in the West Florida Gulf Coast region when the Gulf of Mexico Loop Current spring intrusion (Leipper, 1970) is at its full extent. During such time, the circulation on the open shelf may be strong enough to dominate the bay circulation.

Once the streamfunction becomes known, the sea surface elevation anomaly ζ field can be readily computed from the divergence equation. For a uniform depth ($e=0$), for example,

$$\nabla^2\zeta = d^{-1}\nabla^2\phi - 2d^{-2}\,\mathrm{Ro}(\phi^2{}_{xy} - \phi_{xx}\phi_{yy}), \qquad (3)$$

where ζ is dimensionless and becomes dimensional when multiplied by $C(A_H f)^{\frac{1}{2}}/g$. Eq. (3) is of the Poisson type and can be numerically integrated with the method of successive over-relaxation (SOR). The boundary conditions for ζ are easily obtained from the vertically integrated equation of horizontal motion. The resulting ζ values are of course relative, and the zero is arbitrarily set at one corner $(x=b,\ y=0)$ of the bay.

3. Numerical methods

Eq. (2) can be integrated numerically. The region of interest is divided into 560 square meshes (Fig. 2). Additional grid points just outside the boundary of the region are placed in order to facilitate the central differencing scheme that is used throughout the computation. The centered finite-difference approximation to (2), for a constant d for example, becomes:

$$\begin{aligned}\Delta_x^4\phi_{i,j} + 2\Delta_y^2\Delta_x^2\phi_{i,j} + \Delta_y^4\phi_{i,j} - \gamma(\Delta_x^2+\Delta_y^2)\phi_{i,j} \\ + d^{-1}\,\mathrm{Ro}[\Delta_x\phi_{i,j}(\Delta_y\Delta_x^2\phi_{i,j} + \Delta_y\Delta_y^2\phi_{i,j}) \\ - \Delta_y\phi_{i,j}(\Delta_x\Delta_x^2\phi_{i,j} + \Delta_x\Delta_y^2\phi_{i,j})] = -b^{-1}, \qquad (4)\end{aligned}$$

where the finite difference operators are defined as

$$\begin{aligned}\Delta_x\phi_{i,j} &= (2\Delta x)^{-1}(\phi_{i+1,j} - \phi_{i-1,j}), \\ \Delta_x^2\phi_{i,j} &= (\Delta x)^{-2}(\phi_{i+1,j} + \phi_{i-1,j} - 2\phi_{i,j}), \\ \Delta_x^4\phi_{i,j} &= (\Delta x)^{-4}(\phi_{i+2,j} - 4\phi_{i+1,j} + 6\phi_{i,j} \\ &\qquad - 4\phi_{i-1,j} - \phi_{i-2,j}), \text{ etc.}\end{aligned}$$

The alternating direction implicit (ADI) method is used to solve (4). The proper iterative scheme goes as

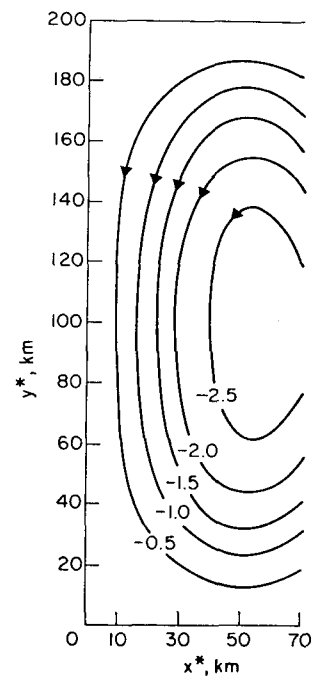

FIG. 3. Computed transport streamlines for $A_H = 10^8$ cm^2 sec^{-1} and flat bottom.

follows:

$$\phi_{i,j}^{n+\frac{1}{2}}=\phi_{i,j}^{n}-r_{n+1}\Delta_x^4\phi_{i,j}^{n+\frac{1}{2}}-2r_{n+1}\Delta_x^2\Delta_y^2\phi_{i,j}^{n}$$
$$-r_{n+1}\Delta_y^4\phi_{i,j}^{n}+\gamma r_{n+1}(\Delta_x^2+\Delta_y^2)\phi_{i,j}^{n}$$
$$-r^{n+1}d^{-1}\,\mathrm{Ro}[\Delta_x\phi_{i,j}^{n}(\Delta_y\Delta_x^2\phi_{i,j}^{n}+\Delta_y\Delta_y^2\phi_{i,j}^{n})$$
$$-\Delta_y\phi_{i,j}^{n}(\Delta_x\Delta_x^2\phi_{i,j}^{n}+\Delta_x\Delta_y^2\phi_{i,j}^{n})]-b^{-1}r_{n+1}, \quad (5)$$

$$\phi_{i,j}^{n+1}=\phi_{i,j}^{n+\frac{1}{2}}-r_{n+1}\Delta_y^4\phi_{i,j}^{n+1}+r_{n+1}\Delta_y^4\phi_{i,j}^{n}. \quad (6)$$

Here, the superscript n represents the number of iteration and r_{n+1} is the iteration parameter which is chosen as

$$r_{n+1}=(0.2)^{1-n}/16, \qquad n=1,\cdots,9$$
$$r_{n+1}=(0.2)^{1-(n-9)}/16, \qquad n=10,\cdots,18,$$
$$r_{n+1}=(0.2)^{1-(n-18)}/16, \qquad n=19,\cdots,27, \text{ etc.}$$

The corresponding finite-difference form for the boundary conditions stated in Section 2 can be expressed in terms of the streamfunction ϕ as follows:

(i) $\phi_{i,j}=0$ and $\phi_{i,j+1}=\phi_{i,j-1}$, for $j=2$ or $j=42$

(ii) $\phi_{2,j}=0$ and $\phi_{3,j}=\phi_{1,j}$

(iii) $\phi_{i,j}=(2/\beta)\phi_{i-1,j}$ and $\phi_{i+1,j}=[2-(\frac{4}{5})\Delta x\alpha]\phi_{i-1,j}/\beta$, where $\beta=2+(\frac{3}{2})\Delta x\alpha$, for $i=16$

(iv) $\phi_{i,j}=0$ and $\phi_{i+1,j}=\phi_{i-1,j}+2\Delta xQ\sin(\pi y/c)$, for $i=16$

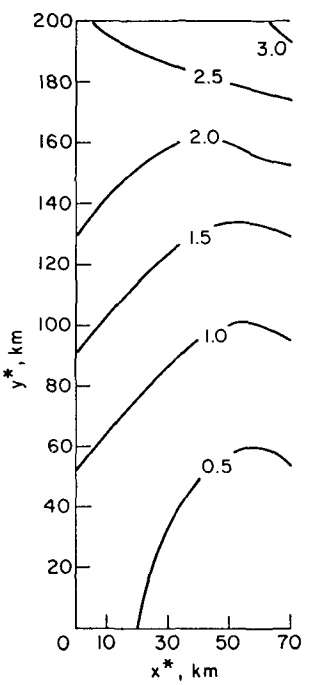

FIG. 4. Computed surface elevation anomlies for $A_H=10^8$ cm^2 sec^{-1} and flat bottom.

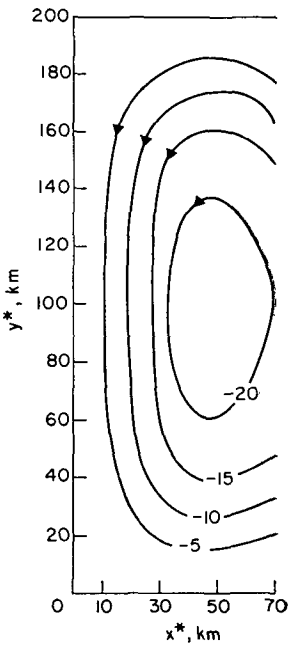

FIG. 5. Computed transport streamlines for $A_H=9\times10^6$ cm^2 sec^{-1} and flat bottom.

Note that during the sweep in the x direction [i.e., Eq. (5)] only the boundary conditions with i fixed, i.e. (ii) and (iii) or (iv), have to be used; and that during the sweep in the y direction, only the boundary conditions with j fixed, i.e. (i), have to be used.

Eqs. (5) and (6) are implicit in $\phi_{i,j}^{n+\frac{1}{2}}$ and $\phi_{i,j}^{n+1}$, respectively, and can be solved efficiently by using algorithms for solving pentadiagonal matrices (von Rosenberg, 1969). This iterative scheme converges quickly. After less than 80 iterations, the fractional difference between two successive steps becomes less than 10^{-9}, i.e.,

$$\mathrm{Max}|(\phi_{i,j}^{n+1}-\phi_{i,j}^{n})/\phi_{i,j}^{n}|<10^{-9}.$$

Using the SOR method for computing ζ from the Poisson equation (3), the iterative finite-difference scheme becomes

$$\zeta_{i,j}^{n+1}=(1-\omega)\zeta_{i,j}^{n}+4^{-1}\omega(\zeta_{i+1,j}^{n}+\zeta_{i-1,j}^{n+1}$$
$$+\zeta_{i,j+1}^{n}+\zeta_{i,j-1}^{n+1})-\omega g_{i,j}(\Delta x)^2/4,$$

where ω is an over-relaxation parameter chosen to be 1.7 and g_{ij} is the finite-difference form of the right-hand side of (3).

4. Results

Computations are performed for a model bay with horizontal dimensions of $b^*=70$ km, $c^*=200$ km. The wind stress amplitude $|T_0^*|$ is taken to be 1 dyn cm^{-2}. The bottom frictional coefficient γ is taken to be 10^{-2}.

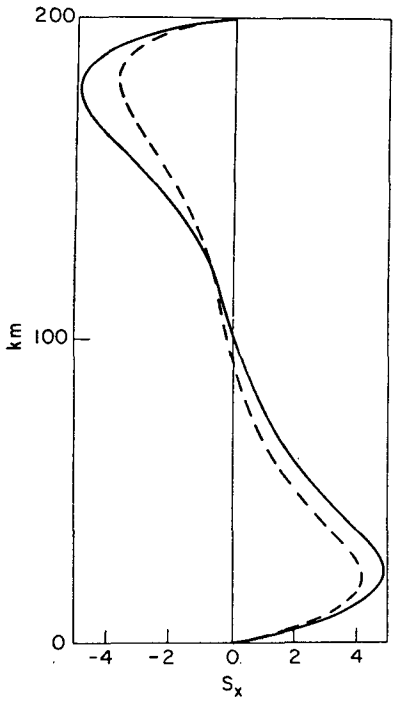

FIG. 6. The comparison between S_x's at the open side of the bay. The solid curve represents $S_x(b, y)$ multiplied by 10 for $A_H=10^8$ cm^2 sec^{-1}. The dashed curve represents $S_x(b, y)$ for $A_H=9\times10^6$ cm^2 sec^{-1}. The bottom is flat.

Its influence is, however, minimal. The positive constant α of proportionality in the boundary conditions at the open side is taken to be 10^{-1}. The vertical eddy viscosity A_V is fixed at 10^2 cm^2 sec^{-1}. Two values of A_H are used: for $A_H=10^8$ cm^2 sec^{-1}, the Rossby number is 0.1 and the flow is essentially linear; for $A_H=9\times10^6$ cm^2 sec^{-1}, the Rossby number is 0.3 and the flow becomes mildly nonlinear.

a. Wind-driven circulation

Considerations are given first to a bay with a uniform depth of 50 m ($a=5$, $e=0$). The fourth term on the left and the second term on the right of (2) are thus identically zero; T_0^* is positive; and boundary conditions (i), (ii) and (iii) are in effect.

1) LINEAR CASE ($A_H=10^8$ cm^2 sec^{-1})

The applied wind-stress torque is essentially balanced by the lateral friction. The streamlines are plotted in Fig. 3 and the sea surface elevation anomalies ζ, which can be computed from the divergence equation once the transports are known, are shown in Fig. 4. The numbers on the streamlines are in units of 10^4 m^3 sec^{-1} and those on the ζ contours are in cm. The circulation pattern in response to a positive wind-stress curl is characterized by the formation of a counterclockwise half-gyre and is symmetrical in the y direction. The flow is largely frictional and crosses the ζ contours. There is little evidence of a geostrophic balance anywhere.

2) NONLINEAR CASE ($A_H=9\times10^6$ cm^2 sec^{-1})

The advection of vorticity becomes measurably important. The frictional effect is important only close to the coast as the width of the bay is now almost 25 times the frictional scale. The streamlines shown in Fig. 5 in units of 3×10^3 m^3 sec^{-1} are slightly more packed to the north (near $y=0$), the direction into which the induced currents flow. A comparison in S_x along the open side with the previous case adequately reflects this distortion (Fig. 6). While the total transport of water exchanged between the bay and the shelf is zero, the largest speed occurs with the outflowing current. It should also be noted in Fig. 5 that, except for the near-coast areas, the y component of the transport appears to be in a geostrophic balance and is directed along the ζ contours plotted in Fig. 7 in units of 0.3 cm.

b. Bathymetry effect

For the purpose of demonstrating how the topography influences the circulation, consider a bay of uniformly sloped bottom in the x direction from 10 m at the coast to 50 m at the open side ($a=1$, $e=4/7$) with $A_H=10^8$ cm^2 sec^{-1}; T_0^* is still positive. The full Eq. (2) is now in effect.

The streamlines as plotted in Fig. 8 show marked asymmetry in the flow pattern with relatively intense outflow in the northern portion. The crowding of

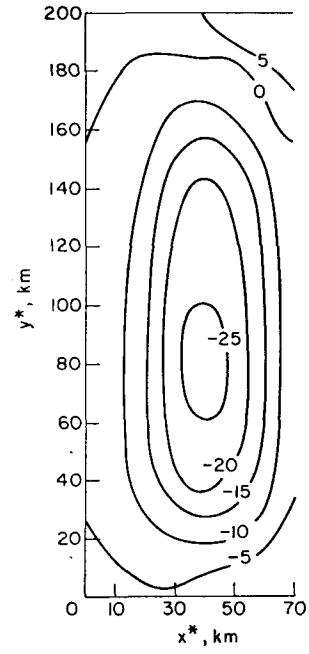

FIG. 7. Computed surface elevation anomalies for $A_H=9\times10^6$ cm^2 sec^{-1} and flat bottom.

streamlines to the north is explained by the fact that at a fixed distance from the coast, the fore-shortening of water columns moving up the slope in the southern portion contributes in the same sense as the lateral diffusion in counteracting the positive wind-stress torque applied by the wind, whereas the stretching of water columns moving down the slope in the northern portion adds to the creation of positive vorticity and demands relatively intensive diffusion from the northern coast for a vorticity balance. For a wind-stress curl in the opposite direction, a similar consideration again leads to the packing of streamlines to the north (near $y=0$). The influence of a uniform continental shelf slope is therefore to distort the flow pattern so that the streamlines become packed to the right of the down slope direction.

c. *Outer shelf-current effect*

To consider the influence of a longshore current, let the alternate set of boundary conditions [(i), (ii) and (iv)] be used with $Q=0.5$ as compared with the maximum S_y of about unity from Fig. 4. The eddy viscosity A_H is kept at 10^8 cm^2 sec^{-1}. Southerly winds (negative T_0*) are assumed. The same law of depth ($a=1, e=4/7$) as in the previous section applies.

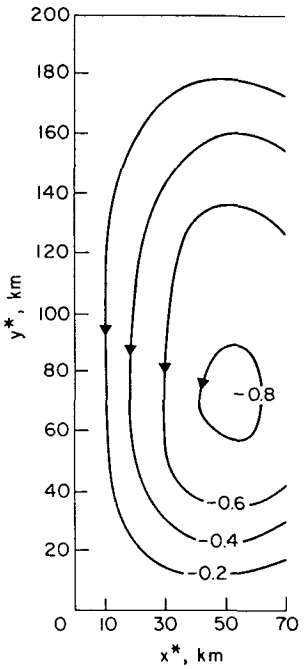

FIG. 8. Computed transport streamlines for $A_H=10^8$ cm^2 sec^{-1} and sloped bottom.

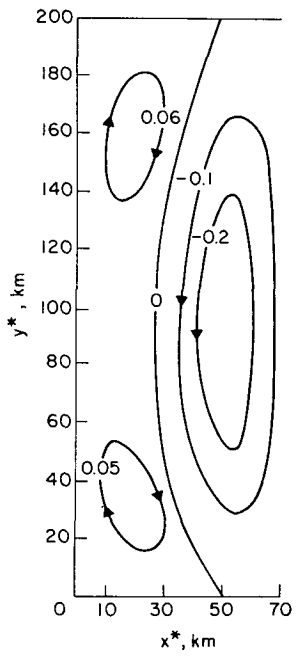

FIG. 9. Computed transport streamlines for $A_H=10^8$ cm^2 sec^1 and sloped bottom. At the open side ($x=b$), $S_x=0$, $S_y=0.5\sin(\pi y/c)$.

The streamlines as plotted in Fig. 9 in units of 10^4 m^3 sec^{-1} show that the circulation pattern is broken into three gyres. The now negative wind-stress curl dominates near the shore and contributes to the formation of two clockwise gyres, one to the north and the other to the south. The influence of the longshore current is confined to the outer portion of the indent and is reflected in the formation of a counterclockwise circulation.

Acknowledgments. The reported research is supported by the Oceanography Section, National Science Foundation, under Grants GA-26563 and GA-29374 and by the Office of Naval Research under Contract N00014-67A-00235-0002 with the Florida State University. It represents a theoretical contribution to CUE (Coastal Upwelling Experiment) which is an IDOE–NSF sponsored project.

REFERENCES

Conte, S. D., and R. T. Dames, 1958: An alternating direction method for solving the biharmonic equation. *Math. Tables, Aids Comput.*, **12**, 195–205.

Leipper, Dale F., 1970: A sequence of circulation patterns in the Gulf of Mexico. *J. Geophys. Res.*, **75**, 637–657.

Rao, Desiraju B., and Tadepalli S. Murty, 1970: Calculation of the steady wind-driven circulations in Lake Ontario. *Arch. Meteor. Geophys. Bioklim.*, **A19**, 195–210.

von Rosenberg, Dale U., 1969: *Methods for the Numerical Solution of Partial Differential Equations*. New York, Elsevier, 128 pp.